Supporting Information

A Water-Soluble Fluorescent Probe Based on Porphyrin Derivative for Cu^{2+} Detection in Aqueous Solution and Living Cells

Jiajun Chen, Chenyang Zhang, Weiye Nie, Lidan Liu, Qi Zhou, and Wenwu Cao**

Center of Acoustic Functional Materials and Applications, School of Materials Science and Intelligent Engineering, Nanjing University, Suzhou 215163, China

*Corresponding author: E-mail: wcao@nju.edu.cn; iquohz@nju.edu.cn

Content

1. Synthesis

The synthetic details of WSPD are described in the following procedures.

1.1. Preparation of 7, 12-Bis(1-bromoethyl)-3, 8, 13, 17-tetramethylporphyrin-2, 18-dipropanoic acid (**1**)

Under nitrogen atmosphere, Hemin chloride (2.0047 g, 3.07 mmol) and 33 *wt.*% hydrogen bromide in acetic acid solution (30 mL) were added into a 100 mL flask and stirred at room temperature for 20 h in the dark. After the reaction, the excess acetic acid solution in the flask was removed under reduced pressure, and then dissolved in acetone (15 mL) and transferred to anhydrous ether (500 mL) to obtain the purplish-black precipitate. The resulting purplish-black products after filtration were collected without purification and dried overnight in vacuum (2.1677 g, yield 97.15%).

1.2 7, 12-Bis [1-(2-(2-hydroxyethoxy) ethoxy)] ethyl-2, 18-dipropionate (2-hydroxyethoxy) ethyl ester-3, 8, 13, 17-tetramethylporphyrin (**WSPD**)

Under nitrogen atmosphere, compound (**1**) (2.1677 g, 2.99 mmol) and diethylene glycol (15 mL, 158.02 mmol) were taken into a 100 mL flask. After the compound (**1**) was completely dissolved, 0.25 mL of H_2SO_4 was added drop by drop, followed by ultrasonic reaction for 1 h, and then stirred for 18 h at room temperature away from light. After the reaction, the saturated $NaHCO_3$ solution (10 mL) was added to neutralize the remaining H_2SO_4. Then, the mixture was poured into 200 mL of *n*-butanol and washed by 200 mL of brine solution and deionized water to remove the residual diethylene glycol. The organic layer was dried over anhydrous sodium sulfate and evaporated to obtain the reddish-brown oil-like crude product, which was purified via column chromatography on silica gel (ethyl acetate: methanol = 4 : 1) to obtain the reddish-brown oil of **WSPD** (0.6514 g, yield 22.26%). ^{1}H NMR (400 MHz, $CDCl_3$, ppm): δ 10.63 – 10.53 (m, 2H, *meso*-H), 10.13,10.12 (s, 2H, *meso*-H), 6.23 – 6.14 (m, 2H, O$\underline{CH}$), 4.45 (t, J = 7.7 Hz, 4H, $\underline{CH_2}CH_2COO$), 4.19 – 4.08 (m, 4H, $COO\underline{CH_2}CH_2$), 3.98 – 3.88, 3.87 – 3.81, 3.80 – 3.74, 3.69 – 3.67, 3.62 – 3.53 (m, 16H, $CHO\underline{CH_2}\underline{CH_2}O\underline{CH_2}\underline{CH_2}OH$), 3.72, 3.70 (s, 6H, $\underline{CH_3}$), 3.67, 3.66 (s, 6H, $\underline{CH_3}$), 3.36 – 3.31 (m, 4H, $CH_2\underline{CH_2}COO$), 3.30 – 3.21, 3.04 – 2.79 (m, 12H,

COOCH$_2$CH$_2$OCH$_2$CH$_2$OH), 2.30 (d, J = 6.6Hz, 6H, CHCH$_3$), -3.74 (s, 2H, pyrrole-H). ^{13}C NMR (100 MHz, $CDCl_3$, ppm) δ 173.40, 173.36, 139.28 – 136.44 (16C, C pyrrole), 98.84, 98.48, 96.97, 96.62, 73.82, 72.53, 72.50, 72.44, 71.95, 71.90, 71.86, 70.86, 68.78, 68.72, 68.65, 68.44, 63.59, 63.17, 61.74, 61.05, 60.93, 60.88, 36.99, 36.94, 29.72, 25.41, 25.08, 21.89, 11.85, 11.77, 11.69, 11.63. FTIR (cm^{-1}): 3381, 3310, 2972, 2917, 2866, 1727, 1648, 1540, 1449, 1413, 1371, 1347, 1292, 1268, 1228, 1166, 1120, 1060, 990, 945, 886, 835, 790, 767, 724, 708, 693, 677. MS (ESI, positive): calcd for $C_{50}H_{70}N_4O_{14}$ $[M+H]^+$: 951.4961. Found: 951.4970. UV-vis: λ_{max}, nm: 390, 503, 535, 568, 620. Elemental Anal. Calcd for $C_{50}H_{70}N_4O_{14}$ (%): C, 63.14; H, 7.42; N, 5.89. Found: C, 63.04; H, 7.39; N, 5.90.

2. Figures and Tables

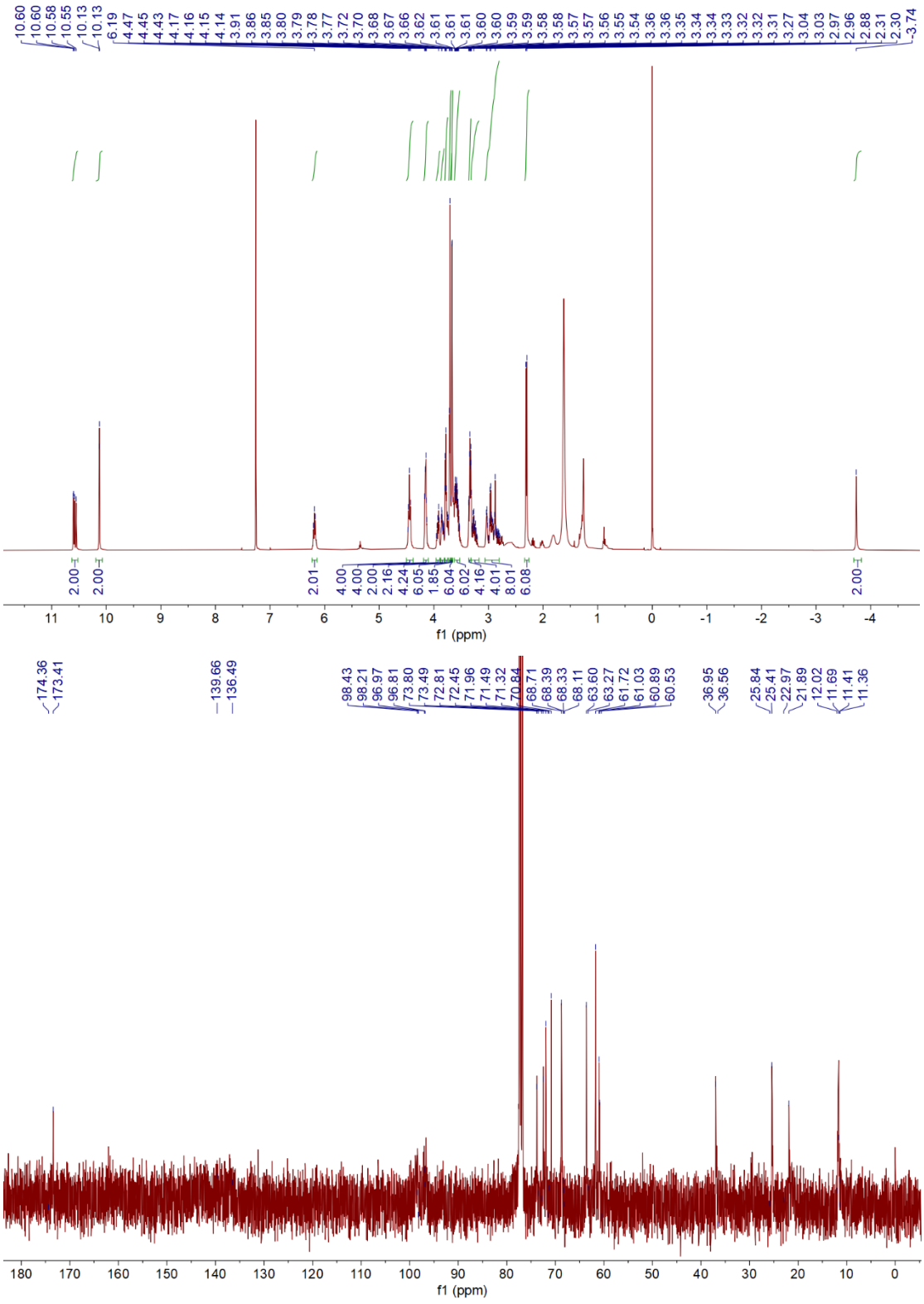

Figure S1. ^{1}H (top) and ^{13}C (bottom) NMR spectra of **WSPD** in deuterated chloroform ($CDCl_3$).

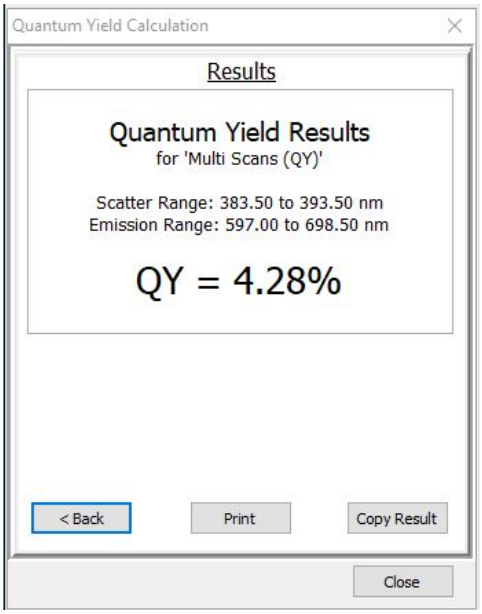

Figure S2. Graph of quantum yield result of the WSPD aqueous solution.

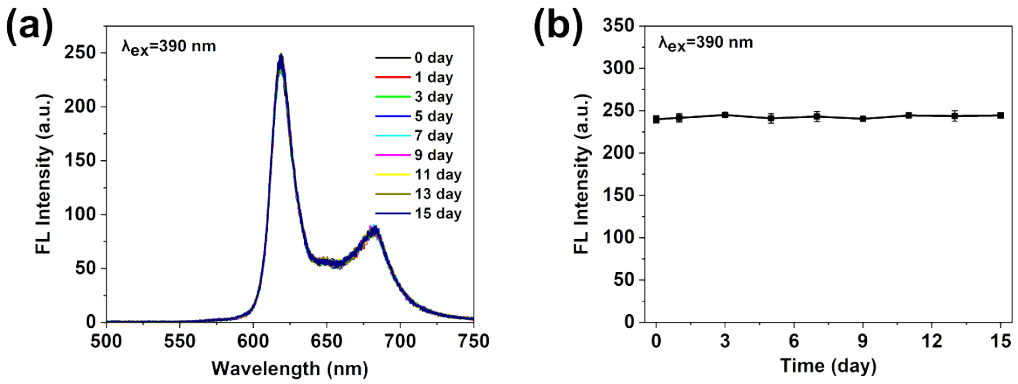

Figure S3. (a) The emission spectra and (b) the fluorescence intensity at 618 nm of WSPD auqeous solution for 15 days.

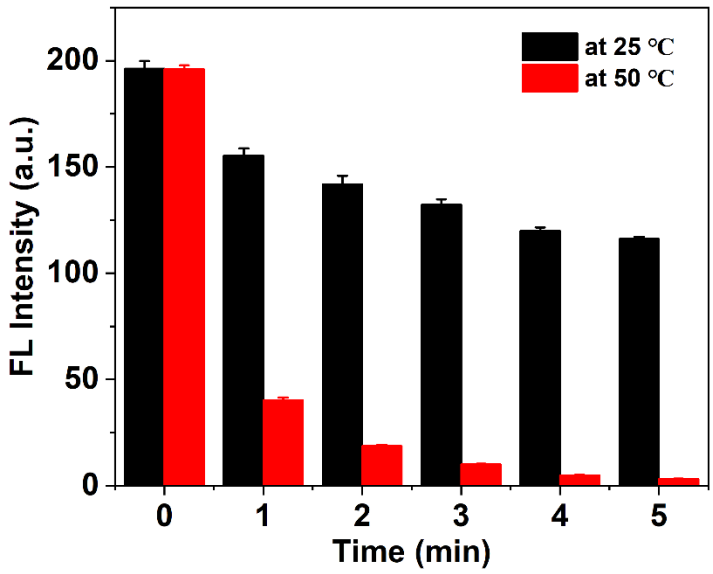

Figure S4. Time-dependent fluorescence responses of WSPD auqeous solution in the presence of Cu^{2+} (10 μM) at 25 ℃ and 50 ℃.

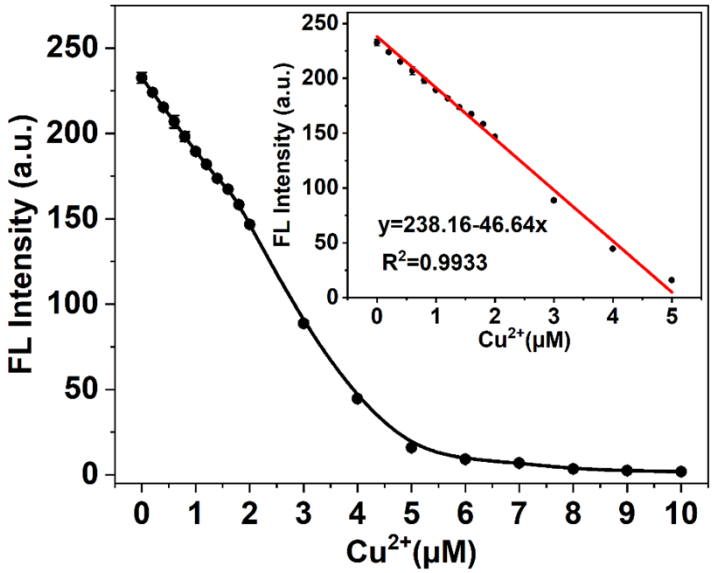

Figure S5. Fluorescence intensities of WSPD aqueous solution at 618 nm after adding different concentrations of Cu^{2+}; inset shows the enlarged plot at Cu^{2+} concentrations from 0 to 5 μM and the linear fit for calculating the limit of detection (LOD).

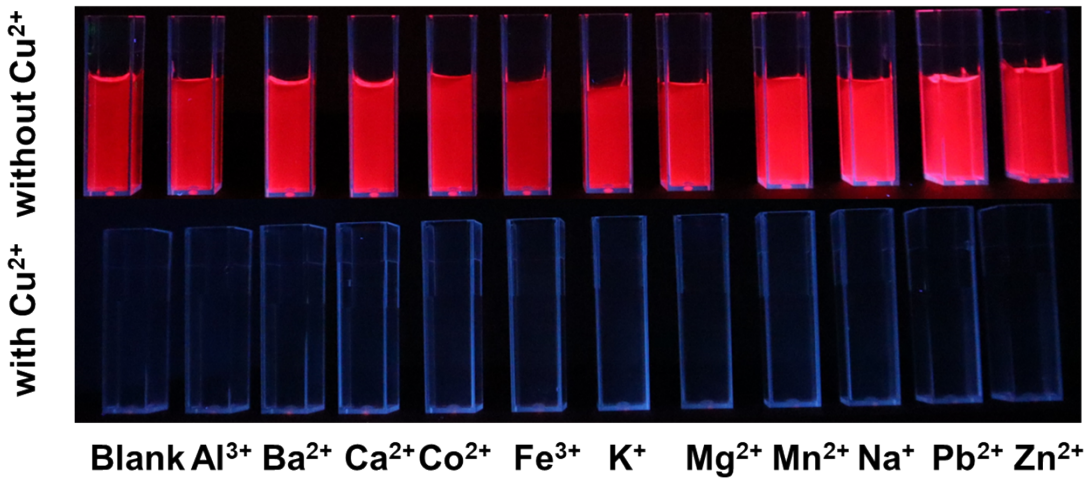

Figure S6. Photographs of WSPD aqueous solutions containing various metal ions under the 365 nm UV lamp, before (top) and after (bottom) adding Cu^{2+} (10 μM).

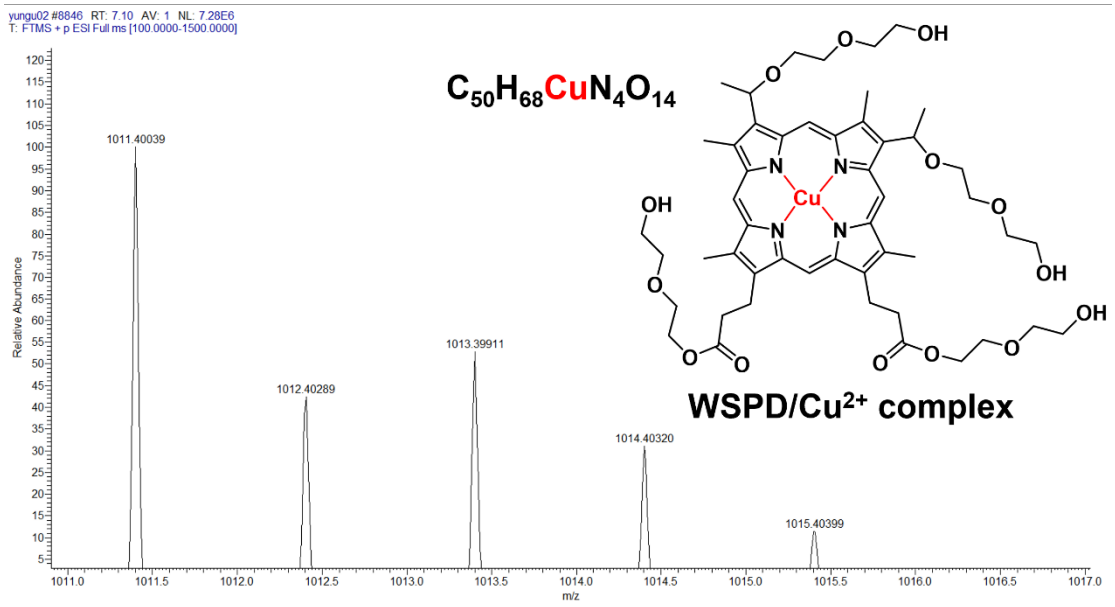

Figure S7. HRMS spectra of WSPD/Cu^{2+} complex ($C_{50}H_{68}CuN_4O_{14}$). MS (ESI, positive): calcd for $C_{50}H_{68}CuN_4O_{14}$ $[M]^+$: 1011.4028. Found: 1011.4004.

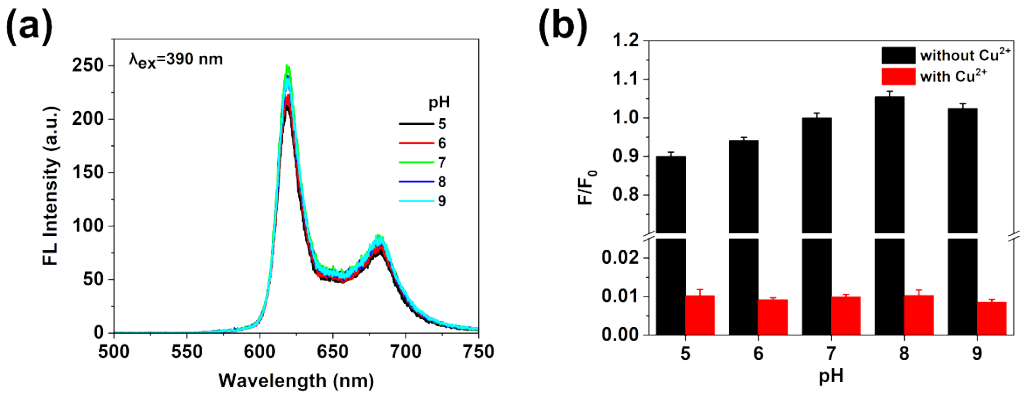

Figure S8. (a) Fluorescence spectra of WSPD aqueous solution at different pH values. (b) Fluorescence responses of WSPD aqueous solution at different pH values, before and after adding Cu^{2+}. F_0 and F are the fluorescence intensities at 618 nm in the absence and presence of Cu^{2+}, respectively.

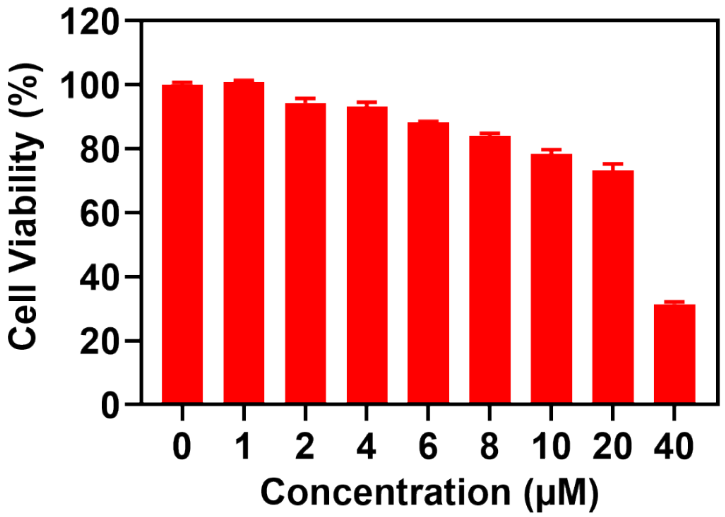

Figure S9. Dependence of WSPD concentration on the cell viability of HT-29 cells after 24 h co-incubation. Data are expressed as the mean ± standard deviation (n = 4).

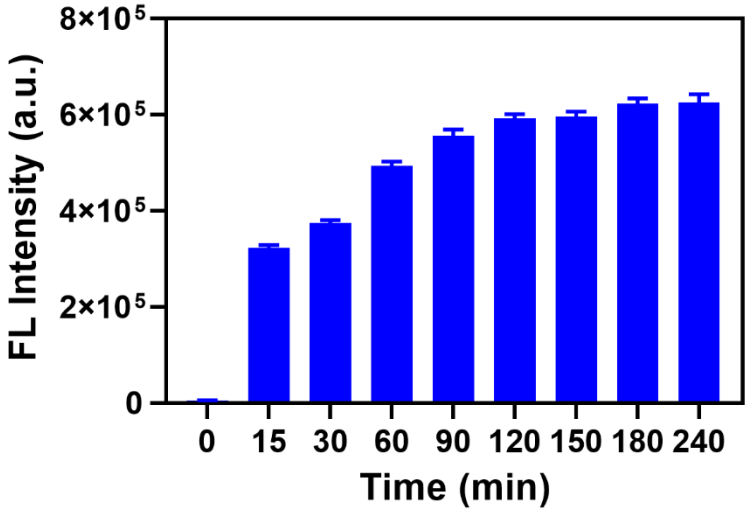

Figure S10. Time-dependent cellular uptake of WSPD in HT-29 cells.

Table S1. Previously reported porphyrin-based sensors for Cu^{2+}detection.

Number	Materials	Detection concentration	Solvent	LOD	Linear range (μM)	R^2	Detection time (min)	Biological application	Year	Ref
1	WSPD	10 μM/ (9.5 μg/mL)	H_2O	6.43 nM	0-1.8 μM	0.9963	5 min	Yes	2025	This work
2	Al-TCPP	100 μg/mL	HEPES buffer	5.28 nM	0-4.76 μM	0.9943	1 min	No	2023	S1
3	ZTMs@FITC	328 μg/mL	H_2O	5.6 nM	0.1-5.0 μM	0.991	30 min	No	2022	S2
4	PTC-1(2H)	1 μM/ (2.65 μg/mL)	THF	6.3 nM	0-4.5 μM	0.99	12 h	No	2022	S3
5	NCPs@PEI	/	H_2O	136 nM	12.5-300 μM	0.999	/	No	2022	S4
6	CQDs	50 μg/mL	PBS buffer	37 pM	0-50 nM	0.983	10 min	Yes	2021	S5
7	PCN222	50 μg/mL	PBS buffer	50 nM	0.4-13 μM	/	3 s	No	2020	S6
8	DCDs	90 μg/mL	PBS buffer	85 nM	0.1-20 μM	0.996	20 min	Yes	2020	S7
9	MOF-525 NPs	5 μg/mL	HEPES buffer	220 pM	1.0-250 nM	0.9981	180 min	Yes	2020	S8
10	HP-GO	10 μg/mL	H_2O	54 nM	0-1.18 μM	0.998	60 min	No	2020	S9

11	ZPSN	2 μM/ (0.621 μg/mL)	PBS buffer	8.2 nM	0-2.0 μM	0.9914	/	Yes	2019	S10
12	UiO-66(OH)$_2$@PCN	50 μg/mL	EtOH and H_2O (v:v = 1:1) mixed solution	0.068 nM	0-1 nM	0.999	/	No	2019	S11
13	TPPS	5 μM/ (4.67 μg/mL)	H_2O	16 nM	0.03-1.0 μM	0.995	/	No	2018	S12
14	ZPA	1 μM	PBS buffer	14.9 nM	0.05-0.75 μM	0.9952	10 min	Yes	2018	S13
15	HCD-TCPP	100 μg/mL	PBS buffer	36 nM	0.2-1.0 μM	0.9946	10 min	Yes	2017	S14
16	Bis-TMPipEOPP	1 μM/ (0.357 μg/mL)	Tris-HCl buffer	8.8 nM	10-300 nM	0.9971	50 min	No	2017	S15
17	MOF-525	6 μg/mL	DMF	67 nM	1.57-18.88 μM	0.9953	40 s	No	2017	S16
18	PCN-222-Pd(II)	/	CH_3CN and H_2O (v:v = 10:1) mixed solution	50 nM	0.05-2 μM	/	30 min	No	2016	S17
19	PS5.M and PpIX	/	HEPES buffer	3.0 nM	0.008-2 μM	0.998	60 min	No	2013	S18

3. Discussion about the comparisons in Table S1

In details, compared with the use of organic solvents, such as No.4, No.12, No.17 and No.18, detection of Cu^{2+} in H_2O using WSPD is more friendly to the environment. In addition, the detection time is another important factor to evaluate the quality of the detection system. Compared with No.9, No.10, No.16 and No.19, the rapid response of WSPD (5 min) can greatly speed up the detection process. More importantly, this sensor has a lower detection concentration (10 μM, 9.5 μg/mL) than No.2, No.3, No.6 – 8 and No.15, and a lower LOD (6.43 nM) than No.5, No.11, No.13 and No.14. Therefore, WSPD is more competitive compared with other reported porphyrin-based sensing systems for Cu^{2+} detection.

4. Determining the limit of detection

The limit of detection (LOD) of WSPD to Cu^{2+} was calculated using linear regression theory,[S19] according to the following equations.

$$S_a = \sqrt{\frac{\sum_{i=0}^{n}(x_i - \bar{x})^2}{n-1}} \#(1)$$

$$S = \frac{\Delta I}{\Delta c} \#(2)$$

$$LOD = \frac{3S_a}{|S|} \#(3)$$

The standard deviation (S_a) regarding the blank solution and the instrument was determined by measuring the fluorescence intensities (x_i) of the solution for 6 times, and calculating the corresponding average intensity ($\bar{x}$). By fitting the intensity data and the average intensity as obtained into equation **(1)**, the value of the standard deviation (S_a) was obtained. Then, a tiny volume of Cu^{2+} stock solution was added into the solution, and the fluorescence intensity was recorded after heating at 50 ℃ for 5 min and then cooling to room temperature. Corresponding variations in intensity (ΔI) and those in Cu^{2+} concentration (Δc) were calculated. By fitting the data into equation **(2)**, the S value for the present system was obtained. Finally, with the values of S_a and S as

determined, the LOD for the system was calculated according to equation **(3)**.

5. References

S1. Y. Liu, L. Guo, Y. Chen, Y. Wang, G. Xu, L. Gu, Z. Yu and Y. Yuan, *J. Environ. Chem. Eng.*, 2023, **11**, 111021.

S2. J. Hou, P. Jia, K. Yang, T. Bu, S. Zhao, L. Li and L. Wang, *ACS Appl. Mater. Interfaces*, 2022, **14**, 13848-13857.

S3. H. Ren, C. Liu, W. Yang and J. Jiang, *Dyes Pigm.*, 2022, **200**, 110117.

S4. S. Li, J. Zhang, Y. Li and Y. Xu, *Dyes Pigm.*, 2022, **200**, 110158.

S5. Y. Liu, F. Seidi, C. Deng, R. Li, T. Xu and H. Xiao, *Sens. Actuators, B*, 2021, **343**, 130072.

S6. Z. Xu, Q. Meng, Q. Cao, Y. Xiao, H. Liu, G. Han, S. Wei, J. Yan and L. Wu, *Anal. Chem.*, 2020, **92**, 2201-2206.

S7. L. Wu, R. Long, T. Li, C. Tang, X. Tong, Y. Guo, S. Shi, H. Xiang and C. Tong, *Anal. Bioanal. Chem.*, 2020, **412**, 7481-7489.

S8. C. Cheng, R. Zhang, J. Wang, Y. Zhang, C. Wen, Y. Tan and M. Yang, *Analyst*, 2020, **145**, 797-804.

S9. F. S. Awad, K. M. AbouZied, A. M. Bakry, W. M. Abou El-Maaty, A. M. El-Wakil and M. S. El-Shall, *Anal. Chim. Acta*, 2020, **1140**, 111-121.

S10. X. Q. Yi, Y. F. He, Y. S. Cao, W. X. Shen and Y. Y. Lv, *ACS Sens.*, 2019, **4**, 856-864.

S11. J. Chen, H. Chen, T. Wang, J. Li, J. Wang and X. Lu, *Anal. Chem.*, 2019, **91**, 4331-4336.

S12. K. Wei, F. Yao and X. F. Kang, *Biosens. Bioelectron.*, 2018, **109**, 272-278.

S13. X. Y. Wang, Z. K. Yu, J. H. Wang, J. Shen, Y. M. Lu, W. X. Shen, Y. Y. Lv and X. Y. Sun, *J. Photochem. Photobio. A Chem.*, 2018, **357**, 49-59.

S14. L. Lu, C. Feng, J. Xu, F. Wang, H. Yu, Z. Xu and W. Zhang, *Biosens. Bioelectron.*, 2017, **92**, 101-108.

S15. K. K. Liu, L. N. Zhang, L. N. Zhu, R. Zhang, X. Z. Li and D. M. Kong, *Sens. Actuators, B*, 2017, **247**, 179-187.

S16. L. Li, S. Shen, R. Lin, Y. Bai and H. Liu, *Chem. Commun.*, 2017, **53**, 9986-9989.

S17. Y. Z. Chen and H. L. Jiang, *Chem. Mater.*, 2016, **28**, 6698-6704.

S18. L. Zhang, J. Zhu, J. Ai, Z. Zhou, X. Jia and E. Wang, *Biosens. Bioelectron.*, 2013, **39**, 268-273.

S19. J. Chen, Z. Fan, C. Zhang, H. Duan and L. J. Fan, *ACS Appl. Polym. Mater.*, 2021, **3**, 2088-2097.